Review Article | Pediatric Imaging

http://dx.doi.org/10.3348/kjr.2015.16.5.973
pISSN 1229-6929 · eISSN 2005-8330
Korean J Radiol 2015;16(5):973-985

Korean Journal of Radiology
KJR

Whole-Body MRI in Children: Current Imaging Techniques and Clinical Applications

Hyun Woo Goo, MD, PhD

Department of Radiology and Research Institute of Radiology, Asan Medical Center, University of Ulsan College of Medicine, Seoul 05505, Korea

Whole-body magnetic resonance imaging (MRI) is increasingly used in children to evaluate the extent and distribution of various neoplastic and non-neoplastic diseases. Not using ionizing radiation is a major advantage of pediatric whole-body MRI. Coronal and sagittal short tau inversion recovery imaging is most commonly used as the fundamental whole-body MRI protocol. Diffusion-weighted imaging and Dixon-based imaging, which has been recently incorporated into whole-body MRI, are promising pulse sequences, particularly for pediatric oncology. Other pulse sequences may be added to increase diagnostic capability of whole-body MRI. Of importance, the overall whole-body MRI examination time should be less than 30–60 minutes in children, regardless of the imaging protocol. Established and potentially useful clinical applications of pediatric whole-body MRI are described.

Index terms: *Whole-body MRI; Infants and children; Tumor; Systemic disease*

INTRODUCTION

Whole-body magnetic resonance imaging (MRI) is useful not only for delineating the extent and distribution of a systemic or multifocal disease but also for making the diagnosis and evaluating treatment responses (1-7). Compared with other whole-body imaging methods, whole-body MRI is inherently advantageous for characterizing soft tissue with good anatomic details. In addition, MRI is particularly useful in children and young adults who require repeated whole-body imaging because it does not use ionizing radiation. In this respect, whole-body MRI is also useful in genetically radiosensitive patients, such as those with neurofibromatosis or ataxia telangiectasia. Several technical developments are worth mentioning that make a whole-body MRI examination practical, including a rolling table platform facilitating continuous acquisition of multiple whole-body MRI stations, a software package enabling seamless composited or merged whole-body images for easier viewing and interpretation, and a dedicated multi-channel, multi-element surface coil system optimizing image acquisition efficiency and signal-to-noise ratio (SNR). As a result, whole-body MRI is increasingly used to image various oncological or non-oncological diseases in children. In this article, the current status of imaging techniques, fundamental and disease-specific imaging protocols, and clinical applications of whole-body MRI in children will be reviewed to boost its widespread use for better patient care.

Received March 29, 2015; accepted after revision May 19, 2015.
Corresponding author: Hyun Woo Goo, MD, PhD, Department of Radiology and Research Institute of Radiology, Asan Medical Center, University of Ulsan College of Medicine, 88 Olympic-ro 43-gil, Songpa-gu, Seoul 05505, Korea.
• Tel: (822) 3010-4388 • Fax: (822) 476-0090
• E-mail: hwgoo@amc.seoul.kr

Imaging Techniques

Whole-body MRI imaging techniques are influenced by magnetic field strength, coil system, and pulse sequence. In general, the SNR and the contrast-to-noise ratio are

greater at 3T than at 1.5T. In contrast, susceptibility artifacts and dielectric shading often degrade whole-body MRI image quality, requiring a large field-of-view at 3T, which can be reduced by using a recently introduced multi-transmit technology (Fig. 1) (5, 8, 9). Furthermore, motion artifacts at thoracoabdominal body parts tend to be more pronounced at 3T. Whole-body MRI signals are received by several coil types, including a quadrature body coil or a multi-channel surface coil. Additional surface coils are not necessary when a quadrature body coil is used, but whole-body MRI image quality improves considerably using a multi-channel surface coil, which allows a higher SNR and spatial resolution. Moreover, scan time can be reduced using a parallel imaging technique with a multi-channel surface coil. A sliding surface coil approach can be used to gain these benefits by using a single conventional torso phased array coil (Fig. 2) (7, 10). A combination of neurovascular and spine coils can be used for whole-body MRI of small children (Fig. 3) (7). Longitudinal coverage for whole-body MRI is shorter, by up to 95 and 125 cm, respectively when using these two approaches (7). However, whole-body MRI using a dedicated multi-channel, multi-element

A B

Fig. 1. 16-year-old boy with testicular rhabdomyosarcoma.
A. Coronal short tau inversion recovery (STIR) whole-body magnetic resonance imaging (MRI) obtained with dual-source parallel radiofrequency excitation technology at 3T reveals residual dielectric shading artifact (arrows) at medial aspect of left buttock and thigh. **B.** Coronal STIR whole-body MRI obtained at 1.5T demonstrates no substantial dielectric shading artifact throughout entire body.

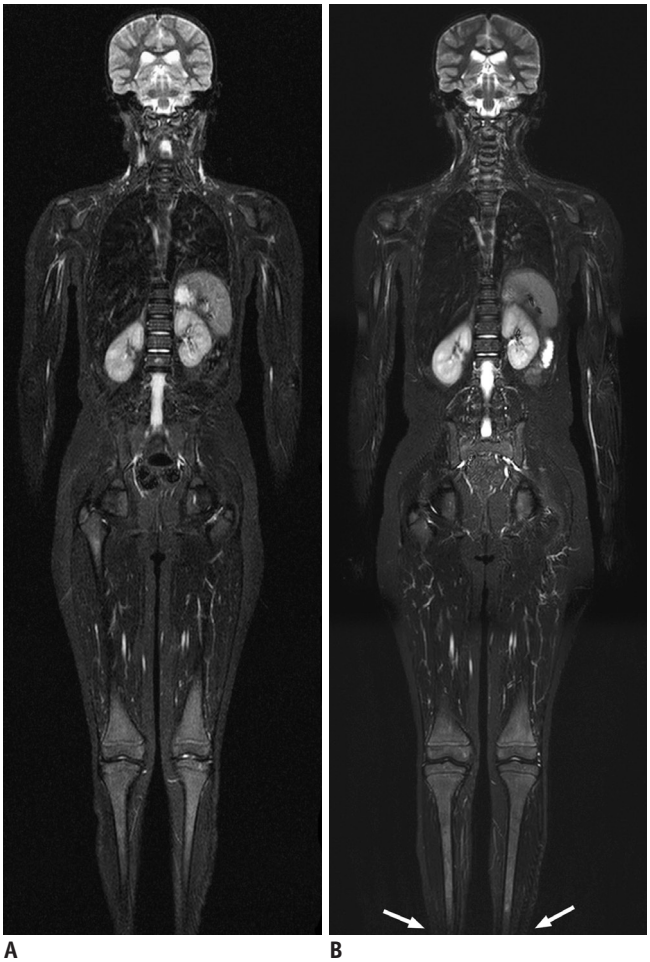

A B

Fig. 2. 11-year-old girl with Ewing sarcoma of cervical spine.
Compared with coronal short tau inversion recovery (STIR) whole-body MRI obtained with quadrature body coil approach at 1.5T **(A)**, coronal STIR whole-body MRI obtained with sliding surface coil approach at 1.5T shows higher signal-to-noise ratio and spatial resolution **(B)**. Longitudinal coverage of sliding surface coil approach is limited by 125 cm. Thus, both legs below low calves (arrows) were not included in this case due to this limitation **(B)**.

Korean Journal of Radiology
KJR

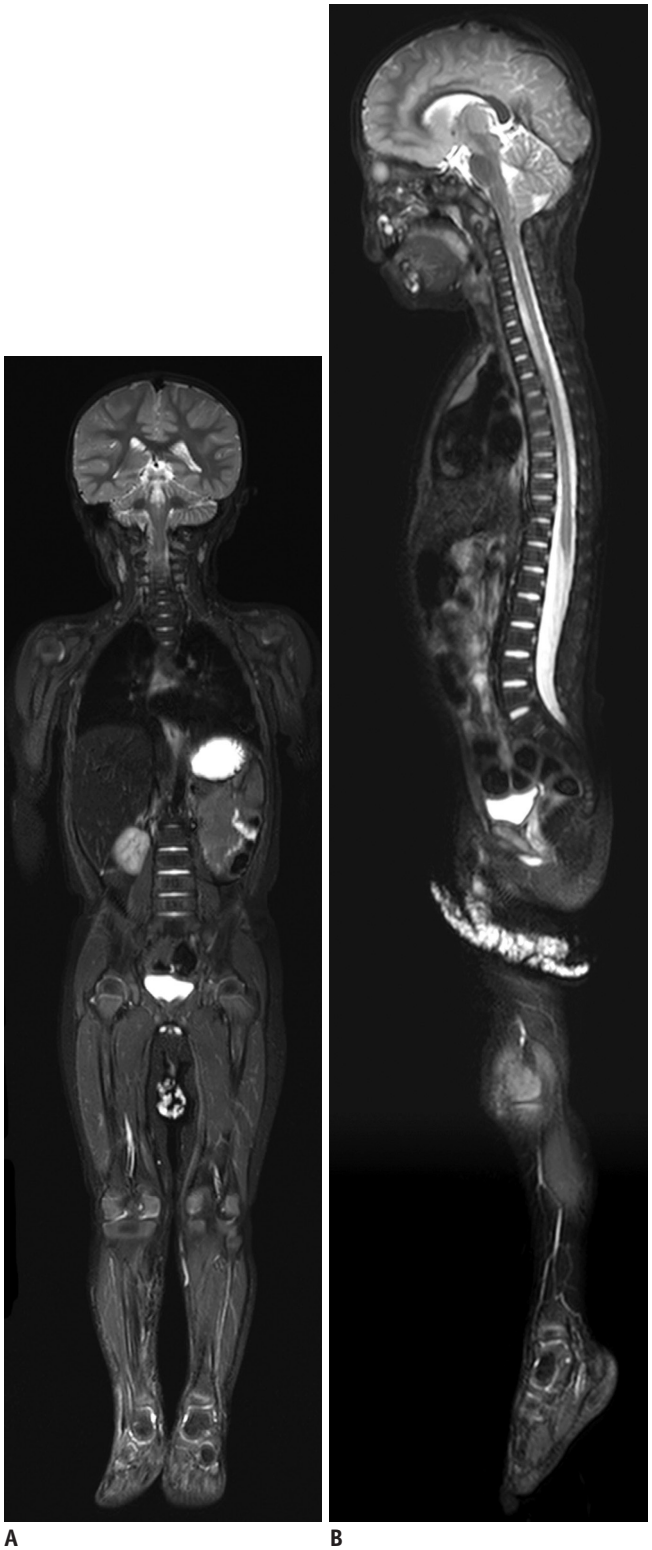

A B

Fig. 3. 2-year-old boy with infantile fibrosarcoma at craniocervical junction.
Coronal **(A)** and sagittal **(B)** short tau inversion recovery whole-body magnetic resonance imaging obtained with combined neurovascular and spine coils at 3T show high signal-to-noise ratio and spatial resolution **(B)**. Spine coils provide high signals sufficient for imaging anterior body parts of this thin, small child.

surface coil system is the current technical standard. Any body part can be imaged at any time during a whole-body MRI examination without moving this coil system. Any pulse sequences can be used for whole-body MRI, and some play a major role due to their ability to cover the whole-body within a short period of time, whereas others play a supplementary role for a specific body part. Short tau inversion recovery (STIR) and T1-weighted sequences are two key pulse sequences used for whole-body MRI.

STIR Imaging

Short tau inversion recovery imaging is most commonly used for pediatric whole-body MRI because the pulse sequence allows lesions to be identified even in the hypercellular red bone marrow common in young children (2-8). Such a lesion tends to be less distinguishable from the red marrow on T1-weighted imaging. STIR imaging provides more homogeneous fat suppression compared to that of fat-saturated T2-weighted imaging, leading to an excellent lesion-to-background contrast ratio but its shortcomings include a lower SNR and a longer scan time. The inversion-preparatory pulse should be adjusted to 150–160 msec at 1.5T and 210–230 msec at 3T to achieve optimal fat saturation on STIR imaging (5, 7, 8). It is noteworthy that osteoblastic or calcified lesions may be barely discernible on STIR images (5, 6).

T2-Weighted Imaging

Frequency-selective fat saturation on T2-weighted images usually results in imperfect fat suppression in body parts showing main static magnetic field (B0) inhomogeneity, such as the neck, lungs, and calves. More uniform fat suppression than that obtained with STIR imaging can be achieved using the recently introduced T2-weighted three-point Dixon technique, which maintains a higher SNR and a shorter scan time (Fig. 4) (11, 12). Moreover, T2-weighted Dixon in-phase images demonstrate anatomic details and fatty marrow changes. It remains to be determined whether this promising new T2-weighted imaging technique will become a mainstay in pediatric whole-body MRI beyond STIR imaging. Fat-water separation or swapping error can rarely occur in one leg or around the thorax (13) regardless of whether two- or three-point Dixon technique and T1 or T2 weighting are used (Figs. 4, 5).

T1-Weighted Imaging

Focal or diffuse bone marrow lesions stand out against

fatty bone marrow on T1-weighted fast spin echo imaging (Fig. 6). Thus, T1-weighted imaging has been commonly included in whole-body MRI examinations of adolescents and adults. One study demonstrated that whole-body three-dimensional (3D) T1-weighted MRI showed as good or better diagnostic performance for metastatic disease screening than that of whole-body two-dimensional (2D) T1-weighted MRI in 30 adult patients with prostate cancer (14). In addition, localized fatty marrow changes after radiation therapy are well-delineated. Lesion enhancement is evaluated using post-contrast fat-saturated 3D T1-weighted gradient echo imaging (Fig. 6). The short scan time of this pulse sequence allows acquiring images during breath-holding. This pulse sequence is often problematic for obtaining uniform fat suppression. The Dixon technique generates four sets of images with different image contrasts, i.e., fat-only, water-only, in-phase, and opposed-phase images, from a single acquisition (Fig. 7). In contrast to fat-saturated 3D T1-weighted gradient echo imaging, water-only images offer almost perfect fat suppression. In addition, marrow-replacing lesions can be distinguished from non-marrow-replacing conditions, including the red marrow, by detecting the absence of significant signal drop on opposed-phase images compared with in-phase images (15). As a result, this pulse sequence with multiple image contrast can be used to enhance lesion detectability on pre- and post-contrast whole-body MRI T1-weighted images (12).

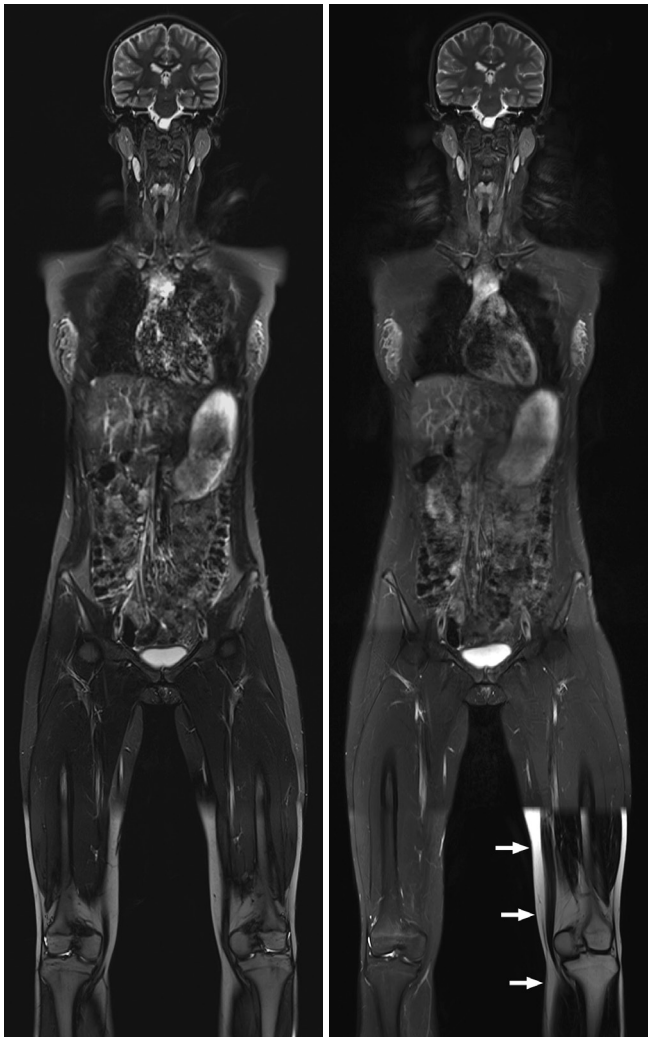

A B

Fig. 4. Advantages of T2-weighted Dixon fast spin echo whole-body magnetic resonance imaging (MRI) in adult volunteer.
Compared with coronal short tau inversion recovery whole-body MRI obtained at 3T showing incomplete fat suppression **(A)**, coronal T2-weighted fast spin echo whole-body MRI with Dixon-based fat saturation at 3T **(B)** clearly demonstrates improved fat suppression throughout entire body except for left leg in lowest station (arrows) caused by fat-water swapping error. Motion artifacts in thorax and upper abdomen are less pronounced on T2-weighted fast spin echo imaging **(B)**.

A B

Fig. 5. 1-year-old boy with neuroblastoma.
Coronal T1-weighted Dixon-based fat-only **(A)** and water-only **(B)** whole-body magnetic resonance imaging at 3T shows that these two image types are swapped at second station covering thoracic region.

Korean Journal of Radiology
KJR

Diffusion-Weighted Imaging (DWI)

Signal intensities (SIs) on diffusion-weighted imaging (DWI) and an apparent diffusion coefficient (ADC) map depend on water diffusion in tissues and, therefore, reflect tumor cellularity. In addition to regional DWI, whole-body DWI is technically feasible and useful for evaluating lymphoma and other small round cell tumors in children (5-7, 16). In addition to staging malignant tumors, whole-body DWI can be used to monitor therapy, e.g., a favorable treatment response is usually accompanied by an increased ADC (Fig. 8) (16, 17).

Diffusion-weighted imaging with background body signal suppression (DWIBS) is commonly used for whole-body DWI because better fat suppression and less image distortion can be achieved throughout the entire body with DWIBS using STIR than DWI using a chemical shift selective

A B

Fig. 6. 14-year-old boy with leukemia.
A. Coronal pre-contrast T1-weighted whole-body magnetic resonance imaging (MRI) at 1.5T shows that majority of normal fatty marrow is replaced by leukemic cells. **B.** Coronal post-contrast fat-saturated T1-weighted MRI at 1.5T reveals not only diffuse abnormal bone marrow enhancement but also extensive osteonecrosis in proximal humeri, distal femurs, and proximal tibias.

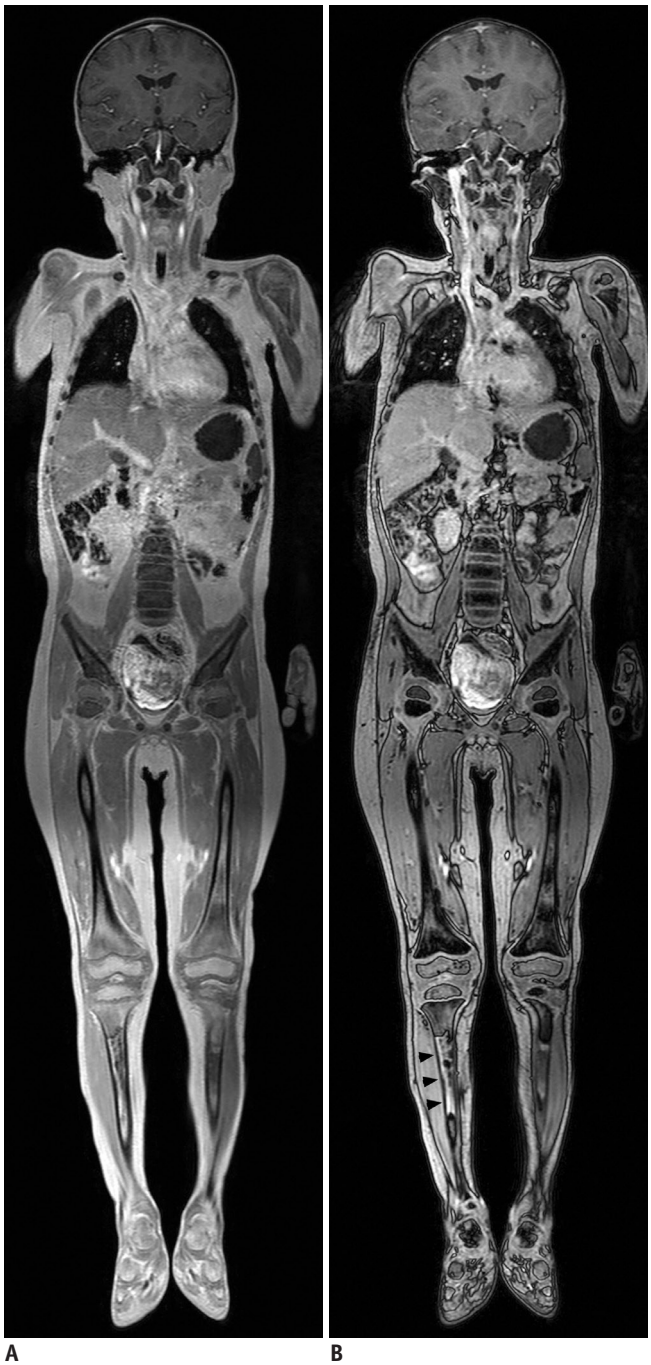

A B

Fig. 7. 4-year-old boy with B-cell lymphoma.
Compared with coronal post-contrast in-phase whole-body magnetic resonance imaging (MRI) at 3T **(A)**, normal bone marrow demonstrates dark signal intensity on coronal post-contrast opposed-phase whole-body MRI at 3T **(B)**. In contrast, marrow-replacing lymphoma lesion in right tibia (arrowheads) remains hyperintense on opposed-phase image **(B)**.

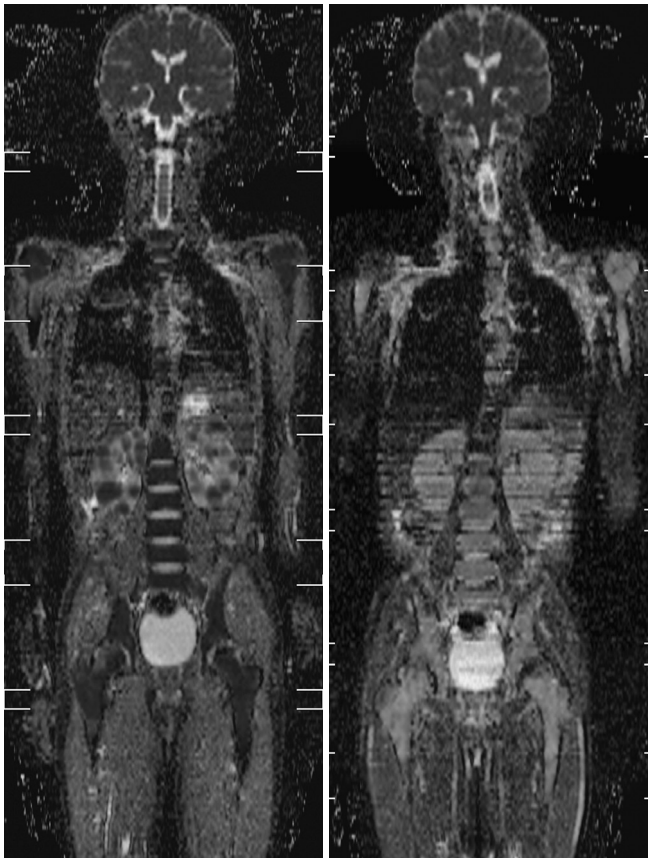

A B

Fig. 8. 10-year-old boy with Burkitt lymphoma.
A. Initial coronal whole-body apparent diffusion coefficient (ADC) map at 1.5T shows restricted water diffusion in all bone marrow and multiple variable-sized renal masses, indicating viable tumors. **B.** Follow-up coronal whole-body ADC map at 1.5T obtained 9 days after induction chemotherapy demonstrates markedly increased water diffusion in lesions suggesting favorable treatment response.

pulse (18). Single-shot echo-planar imaging is mostly used in clinical practice to minimize motion artifacts on DWI. Multi-shot DWI with or without the use of navigator echoes has recently become available and improves spatial resolution and reduces image distortion at the expense of longer acquisition time (19). Notably, DWI acquisition in the axial plane with coronal and sagittal reformations is less vulnerable to image distortion than that of direct coronal or sagittal acquisition. Because of time constraints, the number of b-values for whole-body DWI is usually limited to two. DWI should be acquired over longer times with more b-values. Therefore, it is very difficult to obtain whole-body intravoxel incoherent motion (IVIM) imaging requiring 8–10 b-values within a clinically acceptable time period. Nevertheless, one study demonstrated the technical feasibility of whole-body IVIM imaging in adult volunteers in 72 minutes at 3T (20). However, it remains to be determined whether whole-body IVIM imaging providing diffusion, pseudodiffusion, and perfusion fraction maps has added clinical benefits over whole-body DWI.

Klenk et al. (21) reported that ferumoxytol-enhanced whole-body DWI has equivalent sensitivity and specificity to those of positron emission tomography/computed tomography (PET/CT) for staging 22 young patients with lymphomas and sarcomas. The tumor-to-background contrast is improved effectively with this new imaging technique by signal drop in normal reticuloendothelial system organs, such as the liver, spleen, and bone marrow, after intravenous administration of iron oxide nanoparticles. Moreover, it probably resolves diagnostic pitfalls of whole-body MRI resulting from hypercellular red marrow, which is described in detail later in this article.

Continuously Moving Table MRI

The continuously moving table imaging technique with whole-body coverage can be used for whole-body MRI (Fig. 9) (22) and MR angiography (23). A principal advantage of this technique over the conventional multi-station technique is that the whole-body MRI data are acquired at the isocenter of the magnet where magnetic field inhomogeneity is minimal. High-throughput whole-body MRI examinations can also be achieved with this technique. However, the drawbacks of this technique include numerous axial images resulting in lengthy interpretation and limited longitudinal spatial resolution leading to stair-step artifacts on reformatted images. The latter shortcoming can be ameliorated by using golden angle radial sampling (22). The low-resolution continuously moving table imaging technique can be used to generate a scout view for whole-body MRI or MR/PET.

MR Angiography

Several 3D T1-weighted gradient echo sequence imaging stations adjusted to cover the entire body are used after intravenous administration of a gadolinium-based contrast agent for whole-body MR angiography (24). Instead of the multi-station technique, the continuously moving table imaging technique can be used for whole-body MR angiography, which avoids the stepping artifacts often seen with the multi-station technique (23). The imaging parameters and intravenous injection protocol should be optimized for whole-body MR angiography to minimize the venous contamination frequently seen in the lower extremities. Image quality of whole-body MR angiography

Korean Journal of Radiology
KJR

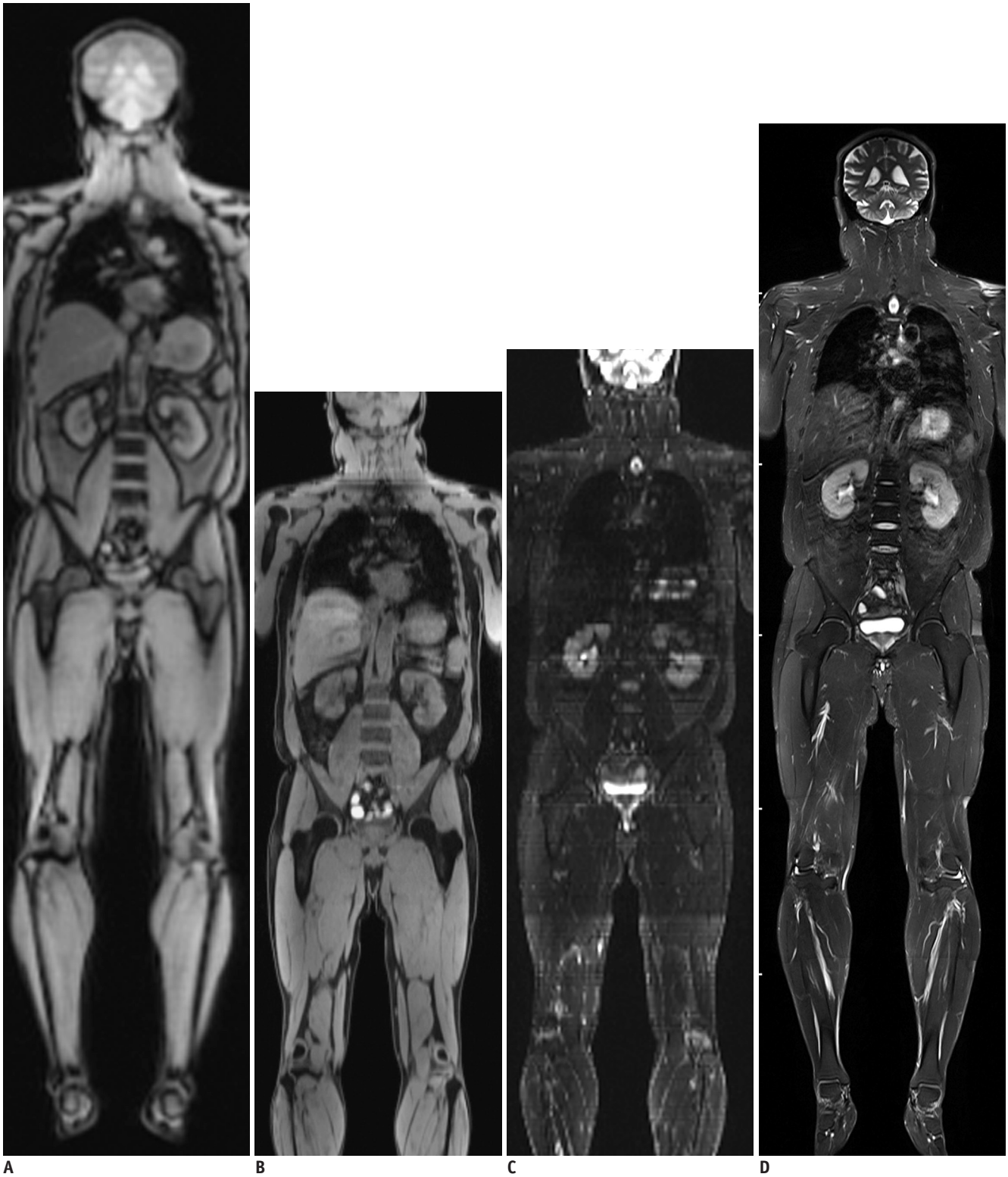

Fig. 9. Whole-body magnetic resonance imaging (MRI) using continuously moving table approach in adult volunteer.
A. Low-resolution coronal reformatted fast gradient-echo whole-body MRI using continuously moving table approach (table feed, 46.9 mm/sec) at 3T was used as scout view for whole-body MRI or MR/positron emission tomography. High-resolution coronal reformatted fat-saturated T1-weighted gradient echo **(B)** and T2-weighted half-Fourier-acquired singe-shot turbo spin echo **(C)** whole-body MRIs using continuously moving table approach at 3T were obtained at much slower table feed (8.9 mm/sec). Compared with coronal Dixon-based fat-saturated T2-weighted fast spin echo whole-body MRI acquired with conventional multi-station approach **(D)**, longitudinal coverage of high-resolution whole-body MRI acquired with continuously moving table approach is slightly limited **(B, C)** and stepping artifacts may degrade image quality **(C)**.

may be compromised by motion and susceptibility artifacts and small vessel size. Systemic vasculopathy in children, such as Marfan syndrome, Loeys-Dietz syndrome, Kawasaki disease, or Takayasu arteritis, can be evaluated using whole-body MR angiography.

Miscellaneous Pulse Sequences

The balanced-steady state free procession sequence has been infrequently used for whole-body MRI (6). This pulse sequence has several merits, including fast scan speed, high SNR, and uniformly high blood pool SI, but it is often limited by off-resonance banding artifacts and high specific absorption rate, particularly at 3T. Pulse sequences dedicated to specific body regions, such as dynamic contrast-enhanced imaging (DCE) and fluid attenuation inversion recovery imaging (Fig. 10), can be added to whole-body MRI examinations as needed.

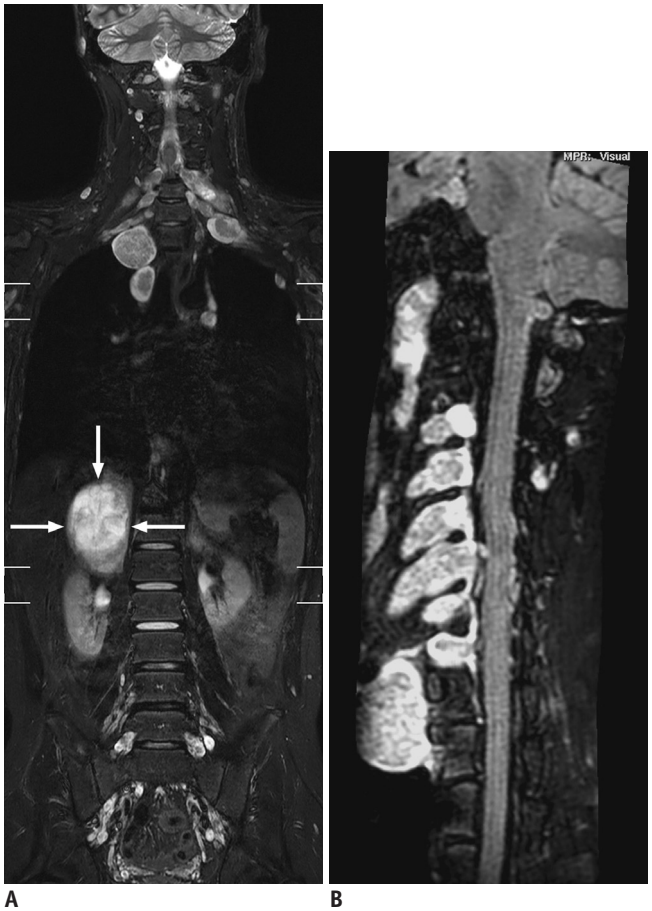

A B

Fig. 10. 15-year-old boy with neurofibromatosis type II and plexiform schwannomas.
A. Coronal short tau inversion recovery whole-body magnetic resonance imaging at 3T shows widespread plexiform schwannomas along nerve roots. Largest lesion (arrows) is noted in right suprarenal region. **B.** Plexiform schwannomas along cervical nerve roots are nicely delineated on curved planar reformatted post-contrast three-dimensional fluid attenuation inversion recovery image at 3T.

Imaging Protocols

The whole-body MRI protocol should be tailored to fit the diagnostic purpose and the patient's condition. In addition to pulse sequences, imagers should determine the scan plane and the necessity for post-contrast imaging. A combination of the coronal and sagittal scan planes is most commonly used. A single coronal scan plane, compared with these two scan planes, may considerably shorten the examination time of whole body MRI at the expense of diagnostic performance (25). The axial plane is the least frequently used scan plane due to lengthy scan and interpretation times. Examination time is also influenced by patient height and scanned longitudinal coverage, i.e., usually from head to toe or infrequently from head to thigh. The 2D scan mode has been commonly used for whole-body MRI but the 3D scan mode with isotropic high spatial resolution and multiplanar reformation is now being increasingly used due to improved scan efficiency and image quality, most frequently for post-contrast T1-weighted imaging. Post-contrast imaging demanding additional examination time is frequently included in the initial examination and intermittently during follow-up examinations. Therefore, a routine whole-body MRI surveillance protocol is usually comprised of pre-contrast coronal and sagittal STIR images only. Overall examination time of whole-body MRI should be less than 30–60 minutes in children because a protracted examination often ends in unsuccessful imaging in these patients. As for other pediatric imaging procedures, sedation or general anesthesia is required for whole-body MRI in young or uncooperative children. A small overlap of 3–5 cm, between adjacent stations during a multi-station imaging protocol, is often placed to create seamless whole-body MRI mainly by compensating for signal loss at the periphery. In addition to the multi-purpose protocol, imagers may develop a dedicated whole-body MRI protocol tailored to a specific disease.

In a recently introduced integrated whole-body MR/PET system, whole-body MRI provided an important anatomic backbone for localizing metabolic abnormalities as well as a Dixon MRI-based attenuation map for correcting the attenuation of PET images (26-28). Approximately 73–80% of the radiation dose can be reduced during MR/

Korean Journal of Radiology
KJR

PET compared with that during PET/CT, which is of critical importance in children (26, 27). In addition, this hybrid system saves total examination time compared with two separate whole-body MRI and whole-body PET examinations. MR/PET offers equivalent lesion detection rates and advantages during a soft tissue evaluation compared with those of PET/CT (27). However, PET standardized uptake values should be carefully compared between MR/PET and PET/CT because an MRI-based PET attenuation correction may result in discrepant values, particularly for bone marrow (13.1%) (27).

Clinical Applications

Whole-body MRI was initially applied to various malignant tumors, except brain tumors, in adults and children (1, 2, 4, 5, 7, 25). Its clinical applications have subsequently expanded to non-oncological diseases. In this section, established and ongoing clinical applications of whole-body MRI and their key results in children are described.

Pediatric Oncology

As mentioned previously, initial tumor staging and the treatment response of pediatric malignant tumors are the most common established clinical applications for whole-body MRI (29). The indisputable advantage of whole-body MRI in pediatric oncology is its lack of ionizing radiation because the high cumulative radiation dose from medical imaging is a major concern in this cohort (30). In general, whole-body MRI is superior to bone scintigraphy for detecting skeletal lesions and exclusively for identifying extraskeletal lesions. Additional DWI and DCE imaging may help improve the limited capability of whole-body MRI for distinguishing viable or recurrent tumors from residual lesions and for evaluating the treatment response (Fig. 8). Given its excellent soft-tissue contrast, whole-body MRI is usually better for evaluating the brain, liver, and bone marrow, whereas PET/CT is relatively superior for assessing the lungs and lymph nodes. It should be recognized that normal bone marrow in children shows a region-specific dynamic pattern of conversion from red (hypercellular hematopoietic) to fatty marrow to avoid potential misinterpretation of pediatric whole-body MRI (31). Conversely, marrow reconversion or hyperplasia may occur in severe anemia or after granulocyte-colony stimulating factor therapy (32). The red marrow tends to be symmetrically distributed and poorly marginated, but it may mimic pathology on T1-, T2-weighted, and STIR sequences. In these cases, opposed-phase imaging helps differentiate marrow lesions from the red marrow.

Several studies have consistently demonstrated that whole-body MRI with or without whole-body DWI offers comparable diagnostic performance to that of PET/CT and, therefore, may be a radiation-free imaging alternative for initial staging of pediatric lymphoma (4, 33). Another study suggested that positive bone marrow lesions on whole-body MRI including whole-body DWI and with a negative blind bone marrow biopsy may have prognostic implications in patients with diffuse large B-cell lymphoma (34). Similar to lymphoma, pediatric small round cell tumors, including neuroblastoma (Fig. 5), Ewing sarcoma (Fig. 2), and rhabdomyosarcoma (Fig. 1), show common histological features, i.e., hypercellularity and a high nucleocytoplasmic ratio. As such, DWI is useful to detect lesions and monitor therapy in patients with these tumors. In contrast, this is not true for carcinomas and Langerhans cell histiocytosis (LCH) with abundant cytoplasm. DCE imaging is particularly useful to assess lesion activity in patients with LCH (3). Because PET is also useful to identify active LCH lesions, a combined analysis with PET and whole-body MRI improves diagnostic accuracy (35). Because most whole-body MRI studies on pediatric small round cell tumors and LCH have been conducted in a small number of patients, further larger studies comparing whole-body MRI with PET/CT and conventional imaging methods are necessary to obtain more conclusive results.

Although whole-body MRI is infrequently used in patients with leukemia, the abnormal marrow replaced by leukemic cells or chloroma can be identified on whole-body MRI (Fig. 6). Furthermore, widespread osteonecrosis in children with leukemia can be detected early on whole-body MRI before articular collapse, which indicates an unfavorable outcome (36). Whole-body tumor burden in patients with neurofibromatosis can be calculated with whole-body MRI-based 3D segmentation and volumetry (Fig. 10) (37). Whole-body MRI may be useful for early detection of associated tumors in cancer predisposition syndromes in children, such as neurofibromatosis type 1, Beckwith-Wiedemann syndrome, multiple endocrine neoplasia, Li-Fraumeni syndrome, von Hippel-Lindau syndrome, and familial adenomatous polyposis (38). In addition, whole-body MRI can be used to find the primary site of an unknown primary tumor.

Pediatric Non-Oncological Diseases or Conditions

The extent and distribution of generalized lymphatic/vascular malformations involving multiple organs or tissues can be evaluated with whole-body MRI. Whole-body MRI is particularly helpful to predict clinical outcome by identifying findings indicating a poor prognosis, such as chylous pleural effusion, mediastinal involvement, and laryngeal involvement in patients with generalized lymphangiomatosis (39).

Whole-body MRI is useful to evaluate disease extent and activity as well as treatment response in patients with juvenile dermatomyositis (Fig. 11) (40). One study (41) reported that whole-body MRI helps recognize characteristic patterns of muscular abnormalities in patients with early onset neuromuscular disorders. Axelsen et al. (42) reported that whole-body MRI is a promising tool for evaluating disease activity and structural damage and is more frequently identified than by clinical examination in

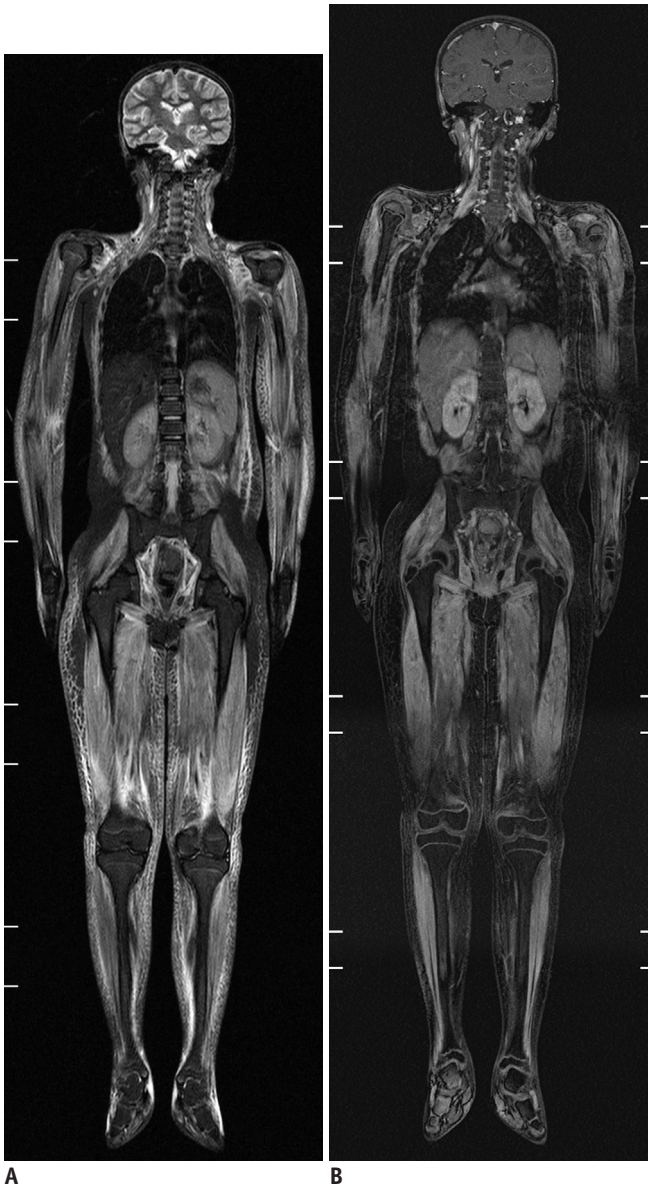

A B

Fig. 11. 10-year-old girl with juvenile dermatomyositis.
A. Coronal short tau inversion recovery whole-body magnetic resonance imaging (MRI) at 1.5T reveals extensive muscular hyperintensity and reticular subcutaneous hyperintensity. **B.** Mild contrast enhancement in active dermatomyositis lesions is shown on coronal post-contrast fat-saturated T1-weighted gradient echo whole-body MRI at 1.5T.

A B

Fig. 12. 6-year-old girl with juvenile rheumatoid arthritis.
Coronal short tau inversion recovery (STIR) post-contrast fat-saturated coronal three-dimensional T1-weighted gradient-echo magnetic resonance image (MRI) at 1.5T. Periarticular soft tissue T2 hyperintensity and enhancement around both shoulder and knee joints (arrows) suggesting active synovitis are identified on STIR **(A)** and post-contrast fat-saturated T1-weighted gradient echo **(B)** whole-body MRIs at 1.5T.

Korean Journal of Radiology
KJR

patients with rheumatoid arthritis. Synovitis indicating active inflammation in patients with juvenile rheumatoid arthritis can be identified as periarticular soft tissue T2 hyperintensity and enhancement on whole-body MRI (Fig. 12). In addition, whole-body MRI may be useful to quantify changes in adipose tissue distribution during medical therapy that coincides with biochemical improvement in patients with familial partial lipodystrophy (43).

Whole-body MRI is useful for detecting chronic recurrent multifocal osteomyelitis, particularly in indeterminate cases, as it shows subclinical edema (44, 45). Whole-body MRI also may be useful to detect an infection focus in children with fever of unknown origin.

In cases with suspected child abuse, whole-body MRI is helpful to identify soft-tissue injuries but insensitive for detecting classic metaphyseal lesions or rib fractures specific to child abuse (46). Of interest, initial experiences of postmortem whole-body MRI have been reported to be a noninvasive complimentary virtual autopsy prior to classic autopsy (47, 48).

Whole-body MRI has been rarely used to assess the extent and distribution of multiple benign bone and soft tissue lesions, such as polyostotic fibrous dysplasia in patients with McCune-Albright syndrome (49), hypophosphatasia (50), Rsai-Dorfman disease (51), and disseminated cysticercosis (52).

CONCLUSION

Whole-body MRI is a useful radiation-free imaging method for evaluating the whole-body extent and distribution of various neoplastic and non-neoplastic diseases in children. Its diagnostic value in children is likely to increase with combined use of functional or metabolic imaging, such as PET, and expanded clinical implications, which remains to be proven by future studies. Pediatric whole-body MRI protocols obviously need to be further optimized towards shorter examination times with better image quality using innovative MRI technologies.

REFERENCES

1. Daldrup-Link HE, Franzius C, Link TM, Laukamp D, Sciuk J, Jürgens H, et al. Whole-body MR imaging for detection of bone metastases in children and young adults: comparison with skeletal scintigraphy and FDG PET. *AJR Am J Roentgenol* 2001;177:229-236
2. Goo HW, Choi SH, Ghim T, Moon HN, Seo JJ. Whole-body MRI of paediatric malignant tumours: comparison with conventional oncological imaging methods. *Pediatr Radiol* 2005;35:766-773
3. Goo HW, Yang DH, Ra YS, Song JS, Im HJ, Seo JJ, et al. Whole-body MRI of Langerhans cell histiocytosis: comparison with radiography and bone scintigraphy. *Pediatr Radiol* 2006;36:1019-1031
4. Punwani S, Taylor SA, Bainbridge A, Prakash V, Bandula S, De Vita E, et al. Pediatric and adolescent lymphoma: comparison of whole-body STIR half-Fourier RARE MR imaging with an enhanced PET/CT reference for initial staging. *Radiology* 2010;255:182-190
5. Goo HW. Whole-body MRI of neuroblastoma. *Eur J Radiol* 2010;75:306-314
6. Chavhan GB, Babyn PS. Whole-body MR imaging in children: principles, technique, current applications, and future directions. *Radiographics* 2011;31:1757-1772
7. Goo HW. Regional and whole-body imaging in pediatric oncology. *Pediatr Radiol* 2011;41 Suppl 1:S186-S194
8. Goo HW. High field strength magnetic resonance imaging in children. *J Korean Med Assoc* 2010;53:1093-1102
9. Willinek WA, Gieseke J, Kukuk GM, Nelles M, König R, Morakkabati-Spitz N, et al. Dual-source parallel radiofrequency excitation body MR imaging compared with standard MR imaging at 3.0 T: initial clinical experience. *Radiology* 2010;256:966-975
10. Takahara T, Kwee T, Kibune S, Ochiai R, Sakamoto T, Niwa T, et al. Whole-body MRI using a sliding table and repositioning surface coil approach. *Eur Radiol* 2010;20:1366-1373
11. Brandão S, Seixas D, Ayres-Basto M, Castro S, Neto J, Martins C, et al. Comparing T1-weighted and T2-weighted three-point Dixon technique with conventional T1-weighted fat-saturation and short-tau inversion recovery (STIR) techniques for the study of the lumbar spine in a short-bore MRI machine. *Clin Radiol* 2013;68:e617-e623
12. Costelloe CM, Madewell JE, Kundra V, Harrell RK, Bassett RL Jr, Ma J. Conspicuity of bone metastases on fast Dixon-based multisequence whole-body MRI: clinical utility per sequence. *Magn Reson Imaging* 2013;31:669-675
13. Schmidt MA. Phase-uncertainty quality map for two-point Dixon fat-water separation. *Phys Med Biol* 2011;56:N195-N205
14. Pasoglou V, Michoux N, Peeters F, Larbi A, Tombal B, Selleslagh T, et al. Whole-body 3D T1-weighted MR imaging in patients with prostate cancer: feasibility and evaluation in screening for metastatic disease. *Radiology* 2015;275:155-166
15. Dreizin D, Ahlawat S, Del Grande F, Fayad LM. Gradient-echo in-phase and opposed-phase chemical shift imaging: role in evaluating bone marrow. *Clin Radiol* 2014;69:648-657
16. Kwee TC, Takahara T, Vermoolen MA, Bierings MB, Mali WP, Nievelstein RA. Whole-body diffusion-weighted imaging for staging malignant lymphoma in children. *Pediatr Radiol* 2010;40:1592-1602; quiz 1720-1721
17. Padhani AR, Makris A, Gall P, Collins DJ, Tunariu N, de Bono JS. Therapy monitoring of skeletal metastases with whole-body diffusion MRI. *J Magn Reson Imaging* 2014;39:1049-

1078
18. Takahara T, Imai Y, Yamashita T, Yasuda S, Nasu S, Van Cauteren M. Diffusion weighted whole body imaging with background body signal suppression (DWIBS): technical improvement using free breathing, STIR and high resolution 3D display. *Radiat Med* 2004;22:275-282
19. Chen NK, Guidon A, Chang HC, Song AW. A robust multi-shot scan strategy for high-resolution diffusion weighted MRI enabled by multiplexed sensitivity-encoding (MUSE). *Neuroimage* 2013;72:41-47
20. Filli L, Wurnig MC, Luechinger R, Eberhardt C, Guggenberger R, Boss A. Whole-body intravoxel incoherent motion imaging. *Eur Radiol* 2015 Jan 10 [Epub]. http://dx.doi.org/10.1007/s00330-014-3577-z
21. Klenk C, Gawande R, Uslu L, Khurana A, Qiu D, Quon A, et al. Ionising radiation-free whole-body MRI versus (18) F-fluorodeoxyglucose PET/CT scans for children and young adults with cancer: a prospective, non-randomised, single-centre study. *Lancet Oncol* 2014;15:275-285
22. Sengupta S, Smith DS, Welch EB. Continuously moving table MRI with golden angle radial sampling. *Magn Reson Med* 2014 Dec 2 [Epub]. http://dx.doi.org/10.1002/mrm.25531
23. Naguib NN, Bohrt K, Nour-Eldin NE, Schulz B, Tawfik AM, Siebenhandel P, et al. Whole-body MR angiography: first experiences with the new TimCT technology with single contrast injection. *J Magn Reson Imaging* 2014;39:434-439
24. Hong TS, Greer ML, Grosse-Wortmann L, Yoo SJ, Babyn PS. Whole-body MR angiography: initial experience in imaging pediatric vasculopathy. *Pediatr Radiol* 2011;41:769-778
25. Siegel MJ, Acharyya S, Hoffer FA, Wyly JB, Friedmann AM, Snyder BS, et al. Whole-body MR imaging for staging of malignant tumors in pediatric patients: results of the American College of Radiology Imaging Network 6660 Trial. *Radiology* 2013;266:599-609
26. Hirsch FW, Sattler B, Sorge I, Kurch L, Viehweger A, Ritter L, et al. PET/MR in children. Initial clinical experience in paediatric oncology using an integrated PET/MR scanner. *Pediatr Radiol* 2013;43:860-875
27. Schäfer JF, Gatidis S, Schmidt H, Gückel B, Bezrukov I, Pfannenberg CA, et al. Simultaneous whole-body PET/MR imaging in comparison to PET/CT in pediatric oncology: initial results. *Radiology* 2014;273:220-231
28. Yoo HJ, Lee JS, Lee JM. Integrated whole body MR/PET: where are we? *Korean J Radiol* 2015;16:32-49
29. Atkin KL, Ditchfield MR. The role of whole-body MRI in pediatric oncology. *J Pediatr Hematol Oncol* 2014;36:342-352
30. Lee E, Goo HW, Lee JY. Age- and gender-specific estimates of cumulative CT dose over 5 years using real radiation dose tracking data in children. *Pediatr Radiol* 2015 Mar 24 [Epub]. http://dx.doi.org/10.1007/s00247-015-3331-y
31. Ording Müller LS, Avenarius D, Olsen OE. High signal in bone marrow at diffusion-weighted imaging with body background suppression (DWIBS) in healthy children. *Pediatr Radiol* 2011;41:221-226
32. Kellenberger CJ, Epelman M, Miller SF, Babyn PS. Fast STIR whole-body MR imaging in children. *Radiographics* 2004;24:1317-1330
33. Littooij AS, Kwee TC, Barber I, Granata C, Vermoolen MA, Enríquez G, et al. Whole-body MRI for initial staging of paediatric lymphoma: prospective comparison to an FDG-PET/CT-based reference standard. *Eur Radiol* 2014;24:1153-1165
34. Adams HJ, Kwee TC, Lokhorst HM, Westerweel PE, Fijnheer R, Kersten MJ, et al. Potential prognostic implications of whole-body bone marrow MRI in diffuse large B-cell lymphoma patients with a negative blind bone marrow biopsy. *J Magn Reson Imaging* 2014;39:1394-1400
35. Mueller WP, Melzer HI, Schmid I, Coppenrath E, Bartenstein P, Pfluger T. The diagnostic value of 18F-FDG PET and MRI in paediatric histiocytosis. *Eur J Nucl Med Mol Imaging* 2013;40:356-363
36. Miettunen PM, Lafay-Cousin L, Guilcher GM, Nettel-Aguirre A, Moorjani V. Widespread osteonecrosis in children with leukemia revealed by whole-body MRI. *Clin Orthop Relat Res* 2012;470:3587-3595
37. Cai W, Kassarjian A, Bredella MA, Harris GJ, Yoshida H, Mautner VF, et al. Tumor burden in patients with neurofibromatosis types 1 and 2 and schwannomatosis: determination on whole-body MR images. *Radiology* 2009;250:665-673
38. Monsalve J, Kapur J, Malkin D, Babyn PS. Imaging of cancer predisposition syndromes in children. *Radiographics* 2011;31:263-280
39. Yang DH, Goo HW. Generalized lymphangiomatosis: radiologic findings in three pediatric patients. *Korean J Radiol* 2006;7:287-291
40. Malattia C, Damasio MB, Madeo A, Pistorio A, Providenti A, Pederzoli S, et al. Whole-body MRI in the assessment of disease activity in juvenile dermatomyositis. *Ann Rheum Dis* 2014;73:1083-1090
41. Quijano-Roy S, Avila-Smirnow D, Carlier RY; WB-MRI muscle study group. Whole body muscle MRI protocol: pattern recognition in early onset NM disorders. *Neuromuscul Disord* 2012;22 Suppl 2:S68-S84
42. Axelsen MB, Eshed I, Duer-Jensen A, Møller JM, Pedersen SJ, Østergaard M. Whole-body MRI assessment of disease activity and structural damage in rheumatoid arthritis: first step towards an MRI joint count. *Rheumatology (Oxford)* 2014;53:845-853
43. McLaughlin PD, Ryan J, Hodnett PA, O'Halloran D, Maher MM. Quantitative whole-body MRI in familial partial lipodystrophy type 2: changes in adipose tissue distribution coincide with biochemical improvement. *AJR Am J Roentgenol* 2012;199:W602-W606
44. Fritz J, Tzaribatchev N, Claussen CD, Carrino JA, Horger MS. Chronic recurrent multifocal osteomyelitis: comparison of whole-body MR imaging with radiography and correlation with clinical and laboratory data. *Radiology* 2009;252:842-851
45. Falip C, Alison M, Boutry N, Job-Deslandre C, Cotten A, Azoulay R, et al. Chronic recurrent multifocal osteomyelitis (CRMO): a longitudinal case series review. *Pediatr Radiol*

2013;43:355-375
46. Perez-Rossello JM, Connolly SA, Newton AW, Zou KH, Kleinman PK. Whole-body MRI in suspected infant abuse. *AJR Am J Roentgenol* 2010;195:744-750
47. Cha JG, Kim DH, Kim DH, Paik SH, Park JS, Park SJ, et al. Utility of postmortem autopsy via whole-body imaging: initial observations comparing MDCT and 3.0 T MRI findings with autopsy findings. *Korean J Radiol* 2010;11:395-406
48. Ross S, Ebner L, Flach P, Brodhage R, Bolliger SA, Christe A, et al. Postmortem whole-body MRI in traumatic causes of death. *AJR Am J Roentgenol* 2012;199:1186-1192
49. Ferreira EC, Brito CC, Domingues RC, Bernardes M, Marchiori E, Gasparetto EL. Whole-body MR imaging for the evaluation of McCune-albright syndrome. *J Magn Reson Imaging* 2010;31:706-710
50. Beck C, Morbach H, Wirth C, Beer M, Girschick HJ. Whole-body MRI in the childhood form of hypophosphatasia. *Rheumatol Int* 2011;31:1315-1320
51. Rittner RE, Baumann U, Laenger F, Hartung D, Rosenthal H, Hueper K. Whole-body diffusion-weighted MRI in a case of Rosai-Dorfman disease with exclusive multifocal skeletal involvement. *Skeletal Radiol* 2012;41:709-713
52. Kumar A, Goenka AH, Choudhary A, Sahu JK, Gulati S. Disseminated cysticercosis in a child: whole-body MR diagnosis with the use of parallel imaging. *Pediatr Radiol* 2010;40:223-227